

RESEARCH PAPER

 OPEN ACCESS 

Knockdown of long non-coding RNA HOTAIR promotes bone marrow mesenchymal stem cell differentiation by sponging microRNA miR-378g that inhibits nicotinamide N-methyltransferase

Wei Wang[#], Tao Li[#], and Shibo Feng

Department of Orthopedics, WuHan HanKou Hospital, Wuhan, Hubei, China

ABSTRACT

Osteoporosis (OP) is associated with a serious social and economic burden. Recent studies have shown that the differential expression of long non-coding RNAs (lncRNAs) is closely related to OP. However, the specific molecular mechanism of HOX transcript antisense intergenic RNA (HOTAIR) remains to be elucidated.

The expression of HOTAIR and miR-378g in OP patients was detected using quantitative reverse transcription polymerase chain reaction (qRT-PCR). Bone marrow mesenchymal stem cells (BMSCs) were isolated and cultured, and osteogenic differentiation was induced. Alkaline phosphatase (ALP) and Runt-related transcription factor 2 (RUNX2) were detected by qRT-PCR, ELISA, and Western blotting. Calcium deposition was measured using Alizarin red s (ARS) staining. Molecular interactions between HOTAIR, miR-378g, and nicotinamide N-methyltransferase (NNMT) were detected using a dual-luciferase reporter assay.

HOTAIR expression was upregulated and miR-378g level was downregulated in OP patients. HOTAIR expression decreased during the osteogenic differentiation of BMSCs. Silencing HOTAIR or NNMT reduced ALP and RUNX2 levels and promoted calcium deposition. The overexpression of HOTAIR or interference with miR-378g inhibited the osteogenic differentiation of BMSCs. HOTAIR negatively regulates miR-378g by targeting NNMT.

HOTAIR is an miR-378g sponge that targets NNMT, inhibits the osteogenic differentiation of BMSCs, and provides a valuable target for the treatment of OP.

ARTICLE HISTORY

Received 21 June 2021

Revised 10 November 2021

Accepted 10 November 2021

KEYWORDS

HOTAIR; miR-378g; differentiation; osteoporosis; osteogenic

Introduction

Osteoporosis (OP), a bone metabolic disease caused by low bone mass and structural damage, has become a global public health problem [1,2]. OP has seriously affected the health and quality of life of patients and increases the economic burden of countries and families [3,4]. Damage to osteoblasts has been reported to be one of the factors leading to the occurrence and development of OP, and bone marrow mesenchymal stem cells (BMSCs) have been proven to have the ability to differentiate into osteoblasts and exert a certain mitigating effect on OP [5,6]. Therefore, it is of clinical value to improve the osteogenic differentiation ability of BMSCs to alleviate OP.

Long non-coding RNAs (lncRNAs) are non-coding transcripts that typically exceed 200

nucleotides in length and are one of the largest and most significantly diverse RNA families that have emerged in recent years [7]. lncRNAs are ubiquitous in many species. In fact, lncRNAs regulate gene expression at the epigenetic, transcriptional, and post-transcriptional levels, and participate in various biological processes [8–10]. lncRNAs have become an intriguing area of research and are widely studied in the diagnosis and treatment of various diseases [11]. Recent reports suggest that lncRNAs play key roles in bone development and disease [12]. For example, the expression of lncRNA-OG is upregulated during osteogenic differentiation and promotes the osteogenic development of BMSCs [13]. The lncRNA, BCAR4, participates in the osteogenic differentiation of BMSCs and exacerbates the

CONTACT Shibo Feng  shibofeng2@163.com  Department of Orthopedics, WuHan HanKou Hospital, No. 7 Erqice Road, Jiangnan District, Wuhan, Hubei 430012, China

[#]The authors contribute equally to this work.

© 2021 The Author(s). Published by Informa UK Limited, trading as Taylor & Francis Group. This is an Open Access article distributed under the terms of the Creative Commons Attribution License (<http://creativecommons.org/licenses/by/4.0/>), which permits unrestricted use, distribution, and reproduction in any medium, provided the original work is properly cited.

progression of OP [14]. HOTAIR is one of the most widely studied maladjusted lncRNAs found in human cancer and has been shown to play a role in pathogenesis, disease progression, drug resistance, and reduced survival [15]. Moreover, the lncRNA, HOTAIR, has been shown to be overexpressed in the serum of patients with OP and inhibits the osteoblastic differentiation of BMSCs in rats [16]. However, the underlying mechanism of HOTAIR in OP remains to be explored.

MicroRNAs (miRNAs) are a class of non-coding RNAs (~22 nucleotides) that play a central role in the post-transcriptional regulation of protein-coding genes through mRNA cleavage, direct translation inhibition, and/or mRNA instability [17]. miRNAs have been reported to participate in the mechanisms of osteoblasts and osteoclasts related to OP [18,19]. For example, miR-335-5p induced the osteogenic differentiation and bone formation of BMSCs in mice and supported the potential application of BMSCs in craniofacial bone regeneration [20]. miR-34a targets NOTCH1 for the healing of tibial defects in irradiated rats and enhanced the osteogenic differentiation of BMSCs [21]. miRNA-378 has been reported to enhance osteogenic differentiation by regulating GalNT7 [22]. Moreover, miR-378g was found to be maladjusted in femoral head necrosis [23]. Nicotinamide N-methyltransferase (NNMT) is an important metabolic enzyme that is overexpressed in human diseases, including Parkinson's disease, cardiovascular disease, cancer, and metabolic disorders [24]. NNMT has been found to be essential for the osteogenic differentiation of BMSCs. Further, NNMT participates in the osteogenic differentiation and bone formation of stem cells, and is upregulated in ovariectomized mice [25,26]. However, the effect of miR-378g/NNMT on osteogenic differentiation and OP has rarely been reported.

We hypothesized that the osteoblastic differentiation of BMSCs could be induced via the regulation of the lncRNA HOTAIR/miR-378g/NNMT signaling pathway to alleviate OP. Functional and mechanistic analysis of BMSCs revealed that HOTAIR upregulated the expression of NNMT through sponge miR-378g, and

then inhibited osteogenic differentiation by reducing osteogenic differentiation-related factors, including ALP, alizarin red staining, and RUNX2. The purpose of this study was to determine the effect of HOTAIR/miR-378g/NNMT on the osteogenic differentiation of BMSCs to provide a research basis for the treatment of OP.

Methods

Clinical samples

Thirty patients with osteoporosis and 30 patients with non-osteoporotic fractures who were admitted to our hospital were enrolled in this study. The participants fasted for 8 h after admission, and 5 mL of blood was intravenously extracted from each patient. After blood coagulation, the supernatant was centrifuged at 1500 g to separate the serum, which was stored for later use. This study was approved by the Ethics Committee of our hospital, and written consent was obtained from all participants prior to blood collection.

Isolation, culture, and differentiation of BMSCs

The animal experiment plan was reviewed and approved by the Animal Care and Use Committee of our hospital. All rats were kept in a specific pathogen-free animal room in the experimental animal research center of our hospital. BMSCs were isolated from the tibia and femur of 10-week-old Sprague-Dawley female rats (weight, 50–60 g) purchased from Hunan SJA Laboratory Animal (China). Briefly, the bone marrow was washed with phosphate buffered saline (PBS) and cultured in α -MEM (Invitrogen, USA) supplemented with 10% fetal bovine serum (FBS), 1% penicillin/streptomycin, and 2-mercaptoethanol (2-ME) at 37°C in an incubator containing 5% CO₂. The culture medium was changed every 3 days to remove free cells. After 5 days, the primary cells were trypsinized and subcultured [27]. When the convergence of the third generation reached 70–80%, the osteogenic differentiation of BMSCs was induced using differentiation medium containing α -MEM, 10% FBS, 100 μ g/mL ascorbic acid, 2 mM β -glycerophosphate, and 10 nM dexamethasone [28].

Table 1. The human primer sequences used for Real-Time PCR.

Gene	Primer sequence
HOTAIR	Forward: 5'-GGGTGTTGGTCTGTGGAAC-3' Reverse: 5'-CAGTGG-GGAACTCTGACTCG-3'
miR-378g	Forward: 5'-ACACTCCAGCTGGGGAAGACTGAGGTTTC-3' Reverse: 5'-CTCAACTGGTGTCTGGAGTCGGCAATTCAGTTGAGAGCCCACT-3'
NNMT	Forward: 5'-AGGAACCAGGAGCCTTTGACT-3' Reverse: 5'-CCTGAGGGCAGTGGATAGG-3'
RUNX2	Forward: 5'-GCCTCAAGGTGGTAGCCC-3' Reverse: 5'-AAGGTGAACTCTTGCCTCGTC-3'
ALP	Forward: 5'-CCTCGTTGACACCTGGAAGAG-3' Reverse: 5'-TTCCGTGCGTTCCAGA-3'
GAPDH	Forward: 5'-CTTGGTATCGTGGAAAGACTC-3' Reverse: 5'-GTAGAGCAGGGATGATGTTCT-3'
U6	Forward: 5'-CGCTTACGAATTTGCGT-3' Reverse: 5'-CTCGCTTCG CAGCACA-3'

Alkaline phosphatase (ALP) activity assay

ALP activity was measured by converting colorless p-nitrophenyl phosphate (pNPP, Sigma, USA) into colored p-nitrophenol. Briefly, after washing twice with PBS, the cells were scraped into a solution containing 20 mM Tris-HCl (pH 8.0), 150 mM NaCl, 2% Triton X-100, 0.02% NAN3, and 1 µg/mL aprotinin. Thereafter, ALP activity at 405 nm was measured with pNPP as a substrate on a spectrophotometer (Agilent Technologies, USA) [29].

Alizarin red S (ARS) staining

The matrix of the BMSCs was evaluated after osteoinduction. Briefly, BMSCs were incubated in 70% ethanol at 25°C for 1 h and then stained with 40 mM ARS for 10 min. The stained BMSCs were photographed using a light microscope (Olympus, Tokyo, Japan) [30].

Quantitative reverse transcription polymerase chain reaction (qRT-PCR)

Total RNA was extracted from blood and cells using the Norgen Biotek Total RNA Purification Kit (Fermentas, USA). RNA was reverse-transcribed using the RevertAid First Strand cDNA Synthesis Kit (Fermentas). qRT-PCR of mRNA was performed on a Bio-Rad iQ5 thermal cycler (Bio-Rad, USA) using SYBR Green Supermix (Bio-Rad). Glyceraldehyde-3-phosphate dehydrogenase (GAPDH) was used as control for HOTAIR, NNMT, ALP, and RUNX2.

The miRNAs in serum samples were collected using the Qiagen miRNeasy Serum/Plasma Kit (Qiagen, Germany). The obtained RNA mixture was eluted in 20 µL RNase-free water and stored at -80°C. Isolation of miRNAs in BMSCs was performed using the mirVana miRNA isolation kit (Ambion, USA). Reverse transcription of miRNA was performed using Ncode miRNA first-strand cDNA synthesis kits (Invitrogen). qRT-PCR was performed on a 7900HT Fast Real-Time System (Applied Biosystems, USA). U6 was used as an endogenous control for miR-378g. The relative expression of each miRNA was determined using the $2^{-\Delta\Delta CT}$ method. The primer sequences are listed in Table 1.

Cell transfection

BMSCs at the exponential stage were used for transfection. Briefly, 1×10^6 cells were cultured in 6-well plates with 2 mL complete medium for 24 h until 90% confluency was achieved. HOTAIR overexpression vector pcDNA-HOTAIR, pcDNA negative control (NC), shRNA (sh)-HOTAIR (sh-HOTAIR 1#, 2#, 3#), sh-NNMT, and sh-NC were acquired from System Biosciences (SBI, USA). antago miR-378g and antagomiR-NC were synthesized by GenePharma (Shanghai, China). Herein, 1000 ng pcDNA, 1000 ng shRNA, 100 nM antago miRNA were transfected into BMSCs using the Lipofectamine 2000 kit (Invitrogen) and cultured according to the manufacturer's instructions [31].

Western blot

Total protein extraction was performed using cell lysis buffer (Ambion), and protein quality was determined using a bicinchoninic acid (BCA) protein assay (Pierce, USA). Briefly, 20 μ g of protein was denatured at 95°C for 10 min in 5% β -mercaptoethanol solution and 95% Laemmli sample buffer (Bio-Rad). After separation by 12% sodium dodecyl sulfate-polyacrylamide gel electrophoresis (SDS-PAGE), the proteins were transferred to nitrocellulose membranes (Schleicher & Schuell, Germany) and blocked for 1 h at 25°C using 0.5% skimmed milk. Thereafter, the membrane was incubated with ALP (ab229126; Abcam, USA), RUNX2 (ab236639; Abcam), and GAPDH (ab8245; Abcam) at 25°C for 1 h, followed by secondary antibodies (Bethyl, USA) at 25°C for 1 h. Membrane-bound antibodies were assessed by chemiluminescence after rinsing with PBS [32].

Luciferase assay

The luciferase assay was performed as previously described [33]. Briefly, starBase was used to detect the binding sites of HOTAIR and miR-378g, and TargetScan was used to identify the binding sites of miR-378g and NNMT. Wild-type (WT) HOTAIR or NNMT containing the putative binding site of miR-378g was amplified and subcloned into the pmirGlo luciferase reporter vector (Ambion). The QuickChange XL Site-Directed Mutagenesis Kit (Stratagene, USA) was used to obtain the mutant HOTAIR (HOTAIR-MUT), the mutant NNMT mutated at three different binding sites (NNMT-MUT1, NNMT-MUT2, NNMT-MUT3), and the mutant NNMT mutated at all three sites (co-MUT). agomiR-378g or agomiR-NC was transfected into BMSCs with wild-type HOTAIR/NNMT or mutant HOTAIR/NNMT using the Lipofectamine 2000 kit. The dual-luciferase reporter system (Promega) and Glomax20/20 luminometer fluorescence detector (Promega) were used to quantify luciferase activity after transfection for 48 h.

Data statistics

Data are expressed as mean \pm standard deviation. One-way analysis of variance (ANOVA) or Student's t-test was used for significance analysis. Statistical analyses were performed using GraphPad Prism version 6. The correlation between HOTAIR, NNMT, and miR-378g in clinical samples was evaluated using Pearson's analysis. Statistical significance was set at $p < 0.05$.

Results

In this study, we hypothesized that the lncRNA, HOTAIR/miR-378g/NNMT, plays a biological role in OP and the osteogenic differentiation of BMSCs. HOTAIR, miR-378g, and NNMT were designated as genes of interest through bioinformatics analysis. Clinical monitoring and functional loss-gain analysis showed that HOTAIR, miR-378g, and NNMT are involved in BMSC osteogenic differentiation and are associated with OP. Mechanistic analysis showed that HOTAIR, as a ceRNA, upregulated NNMT via sponge miR-378g, and thus significantly inhibited BMSC osteogenic differentiation.

HOTAIR/miR-378g/NNMT axis in osteoporosis

HOTAIR has been reported to inhibit osteogenic differentiation, suggesting its osteoporosis-promoting effect [16]. However, the ceRNA mechanism involving HOTAIR has not been reported for osteoporosis. We uploaded the 109 differentially expressed genes in osteoporosis from GSE35959 to STRING 11.0 for protein-protein interaction analysis, and protein-protein interaction was visualized using Cytoscape. Sixty-six of the 109 genes were found to be closely associated. NNMT1 showed close interactions with KCNJ10, ADAM12, and EPHA3 (Figure 1(a)). NNMT1 was significantly upregulated in OVX-induced osteoporosis [26]; however, its role in osteoporosis has not been studied. By intersecting the target miRNAs of HOTAIR, the target miRNAs of NNMT, and the DE-miRNAs of GSE91033, we identified miR-378g as a potential miRNA that linked HOTAIR and NNMT in osteoporosis (Figure 1(b)).

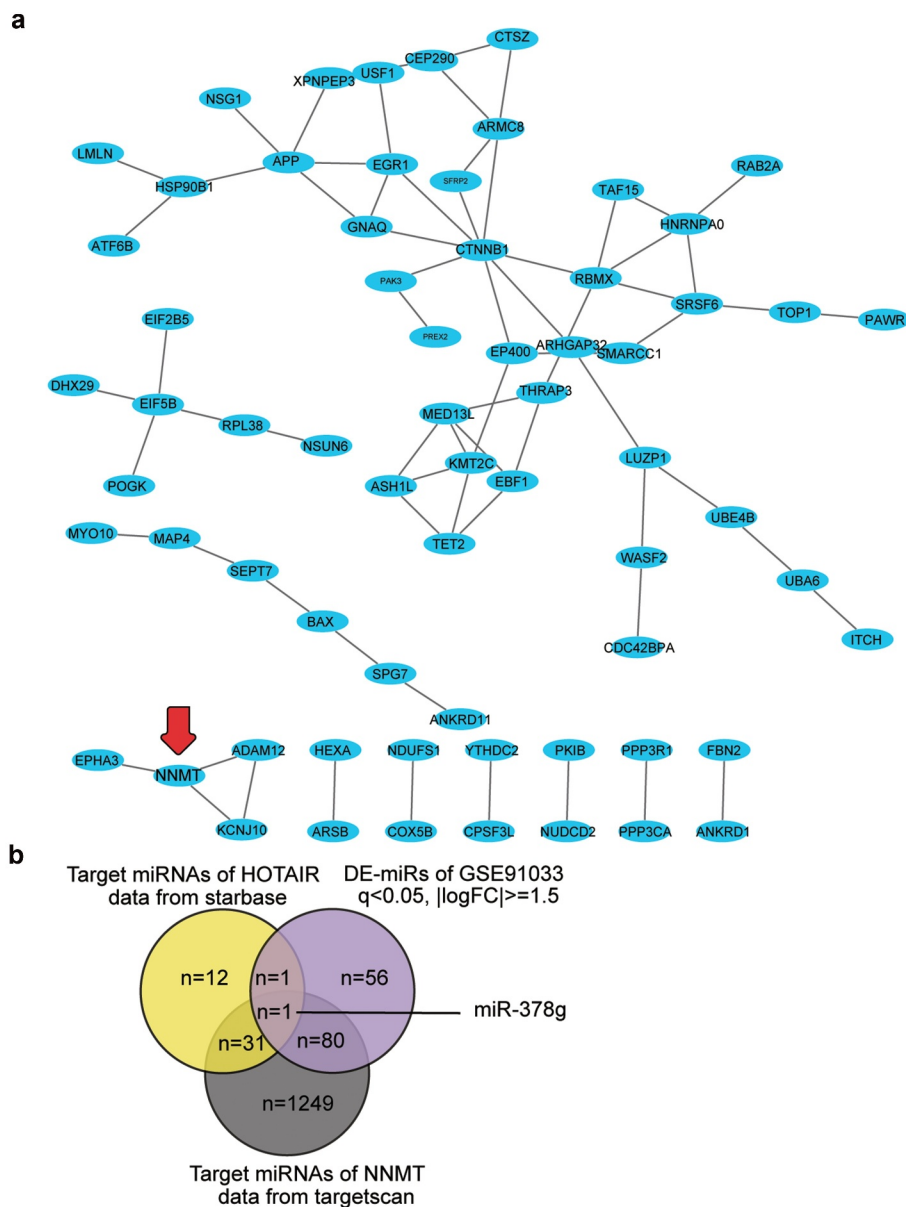


Figure 1. HOTAIR/miR-378g/NNMT axis may be involved in osteoporosis. (a) Protein–protein interaction analysis of the significantly upregulated genes of GSE35959 data series (adjusted $P < 0.05$ and $\log FC \geq 2$, $n = 109$) by string algorithm. (b) The intersection between the target miRNAs of HOTAIR, the target miRNAs of NNMT, and the differentially expressed miRNAs in osteoporosis (GSE91033 data). The target prediction of HOTAIR was conducted using the starBase algorithm, while that of NNMT was conducted using the TargetScan algorithm. The DE-miRNAs of GSE91033 were analyzed using the criteria of adjusted $P < 0.05$ and $|\log FC| \geq 1.5$.

HOTAIR is highly expressed in OP and is associated with osteogenic differentiation

To explore the effect of HOTAIR on osteoporosis, qRT-PCR was used to determine HOTAIR expression in the sera of patients. HOTAIR expression in OP patients was found to increase by approximately threefold relative to that in normal patients (Figure 2(a)). Such finding indicates that HOTAIR

may be related to OP. BMSCs were then used as the research object to induce osteogenic differentiation to observe the mechanism of HOTAIR. The morphology of cells was observed on day 4 after osteogenic differentiation. Accordingly, the cells were found to grow well and displayed spindle growth (Figure 2(b)). ARS staining is often used to detect osteoblast differentiation [34]. Therefore, ARS staining was used to observe the calcium nodules after

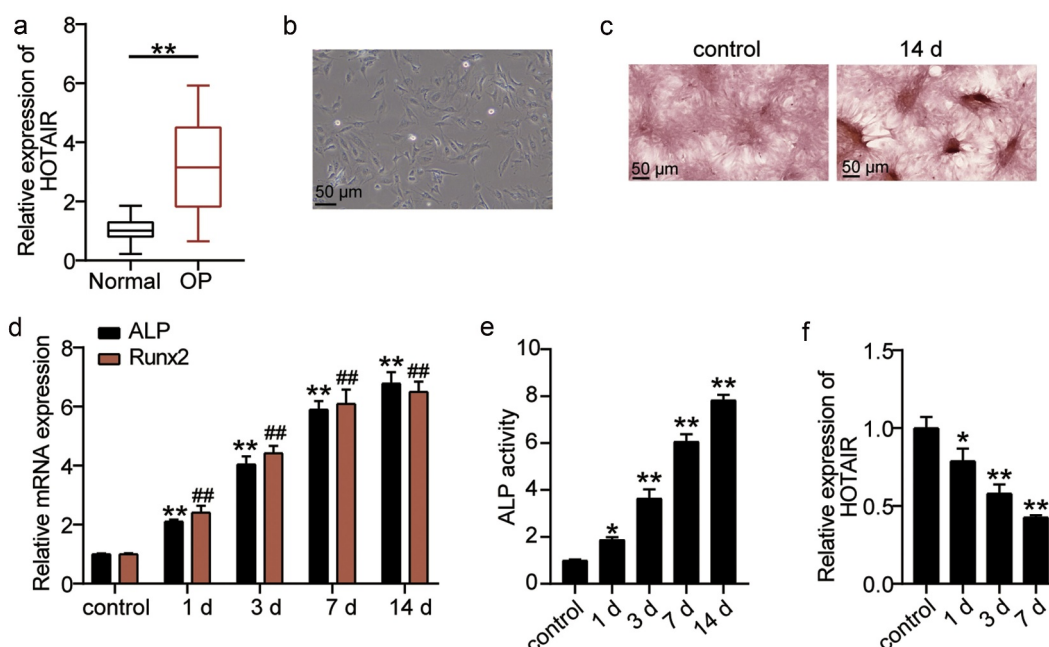


Figure 2. The relationship between HOTAIR expression level and osteogenesis. (a) HOTAIR expression levels in the serum of patients with non-osteoporotic bone fractures (normal) or osteoporosis (OP). $**P < 0.001$. (b) The shape of BMSCs on day 4 of osteogenic differentiation. (c) Following culture in osteogenic induction medium for 14 days, BMSCs exhibited more mineralized nodules according to Alizarin Red S staining. (d) The expression levels of the osteoblast marker genes, *ALP* and *RUNX2*, on different days of induction. $**P < 0.001$ vs. control in *ALP*. $##P < 0.001$ vs. control in *RUNX2*. (e) *ALP* activity on different days of induction. $**P < 0.001$ vs. control. (f) The expression of HOTAIR on different days of induction. $*P < 0.05$, $**P < 0.001$ vs. control. BMSCs, Bone mesenchymal stem cells; HOTAIR, X-inactive specific transcript; *ALP*, alkaline phosphatase; *RUNX2*, runt related transcription factor 2. Data are expressed as mean \pm standard error. In Panels D-F, one-way analysis of variance was used for data analysis, followed by Dunnett's post hoc test. In Panel A, unpaired t-test was used for data analysis. The experiment was repeated three times.

osteogenic differentiation. Calcium deposition was found to be significant at 14 days after induction (Figure 2(c)). *Runx2* is a key regulator of the osteoblast lineage and induces the maturation of osteoblast phenotypes [35]. *ALP* is a marker enzyme of mature osteoblasts, reflecting its osteogenic differentiation ability [36]. Hence, the expression levels of *ALP* and *RUNX2*, the key genes involved in osteogenic differentiation, were measured. The levels of *ALP* and *RUNX2* increased with the time of osteogenic differentiation (Figure 2(d)). *ALP* activity was determined by ELISA, which confirmed that with the extension of osteogenic differentiation time, *ALP* activity increased (Figure 2(e)). Such finding indicated that BMSCs differentiated into osteoblasts. Furthermore, the level of HOTAIR expression during the osteogenic differentiation of BMSCs was measured, showing that HOTAIR expression decreased with differentiation time (figure 2(f)).

Such finding suggests that HOTAIR is also involved in osteogenic differentiation.

Downregulation of HOTAIR promotes the osteogenic differentiation of BMSCs, while upregulation of HOTAIR inhibits BMSC osteogenic differentiation

We attempted to elucidate the mode of action of HOTAIR on the osteogenic differentiation of BMSCs. Abnormal regulation of HOTAIR expression in BMSCs showed that the HOTAIR expression levels in the sh-HOTAIR 1#, sh-HOTAIR 2#, and sh-HOTAIR 3# groups were reduced by approximately 40%, 60%, and 30%, respectively, compared with the sh-NC group (Figure 3(a)). Such finding indicates that HOTAIR expression in BMSCs was successfully knocked down and sh-HOTAIR 2# was selected for follow-up

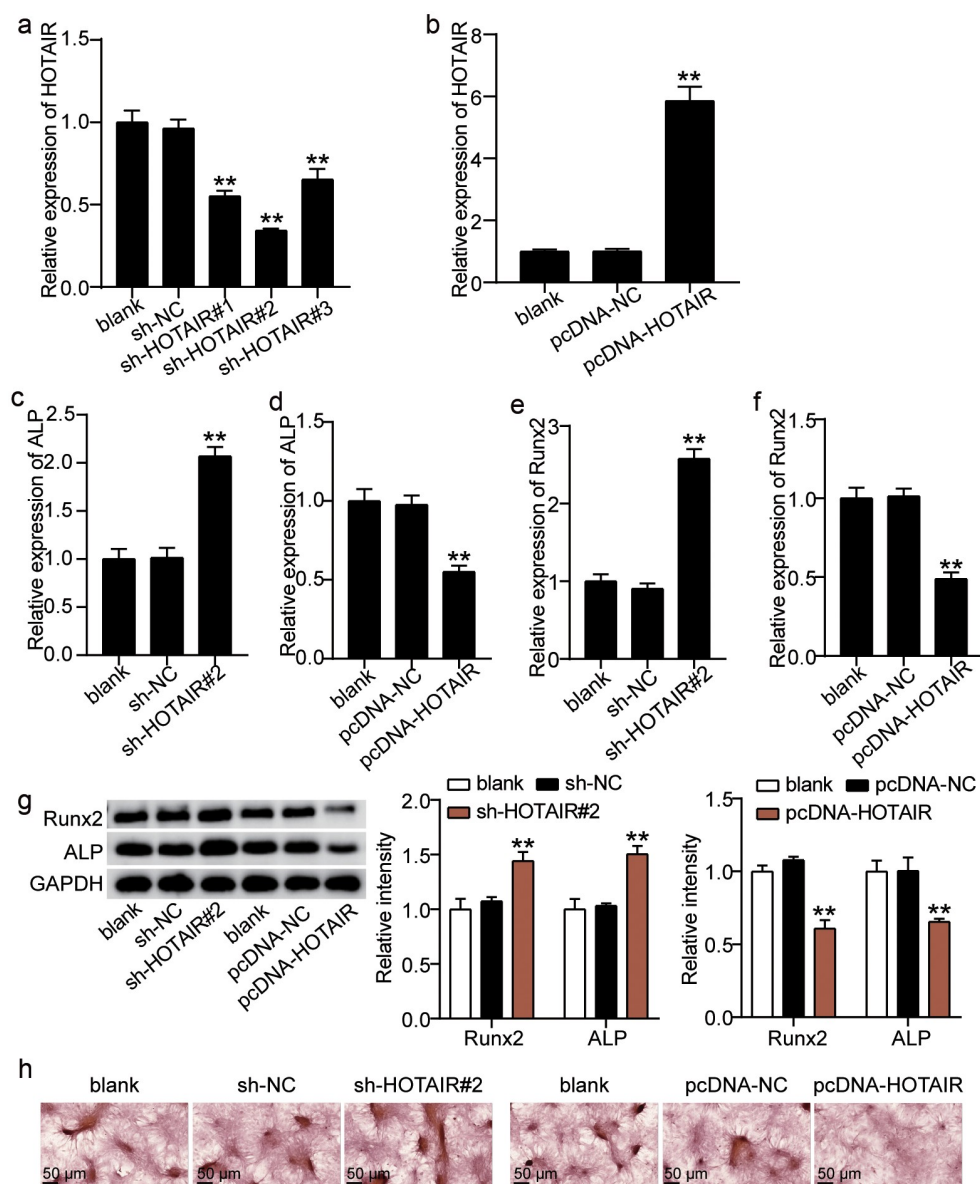


Figure 3. Effect of HOTAIR expression on osteogenesis. (a) HOTAIR expression in BMSCs treated with sh-NC, sh-HOTAIR 1#, sh-HOTAIR 2#, or sh-HOTAIR 3# detected by qRT-PCR. ** $P < 0.001$ vs. sh-NC. (b) HOTAIR expression in BMSCs treated with pcDNA-NC or pcDNA-HOTAIR detected by qRT-PCR. ** $P < 0.001$ vs. pcDNA-NC. (c) ALP expression in BMSCs treated with sh-NC or sh-HOTAIR 2# detected by qRT-PCR. (d) ALP expression in BMSCs treated with pcDNA-NC or pcDNA-HOTAIR detected by qRT-PCR. (e) RUNX2 expression in BMSCs treated with sh-NC or sh-HOTAIR 2# detected by qRT-PCR. (f) RUNX2 expression in BMSCs treated with pcDNA-NC or pcDNA-HOTAIR detected by qRT-PCR. (g) The protein expression of ALP and RUNX2 in BMSCs treated with sh-HOTAIR 2# or pcDNA-HOTAIR measured by Western blot analysis. (h) The mineralized nodules of BMSCs treated with sh-HOTAIR 2# or pcDNA-HOTAIR measured by Alizarin Red S staining. (c-g) ** $P < 0.001$ vs. blank. BMSCs, Bone mesenchymal stem cells; HOTAIR, X-inactive specific transcript; ALP, alkaline phosphatase; RUNX2, runt related transcription factor 2. pcDNA-HOTAIR, HOTAIR overexpression vector; pcDNA-NC, negative control of HOTAIR overexpression vector; sh-HOTAIR, shRNA of HOTAIR; sh-NC, negative control of shRNA. Data are expressed as mean \pm standard error. One-way analysis of variance was used for data analysis, followed by Dunnett's post hoc test. The experiment was repeated three times.

experiments. After the overexpression of HOTAIR, the expression level of HOTAIR in BMSCs increased by approximately sixfold (Figure 3(b)). Thus, we proceeded to explore the effect of changes in HOTAIR on ALP and RUNX2.

ALP and RUNX2 expression levels were found to increase by 2.0- and 2.5-fold, respectively after silencing HOTAIR, and decrease by 45% and 50% after increasing HOTAIR (Figure 3(c-f)). In addition, Western blot analysis showed that the

RUNX2 and ALP expression of sh-HOTAIR 2# was 1.4- and 1.6-fold higher than that of sh-NC, respectively, while the overexpression of HOTAIR reduced the expression levels of ALP and RUNX2 to 40% and 35% of the pcDNA-NC group, respectively (Figure 3(g)). ARS staining also showed that calcium deposition increased after the transfection of sh-HOTAIR 2# into BMSCs but was inhibited after BMSCs were transfected with pcDNA-HOTAIR (Figure 3(h)). Such finding suggests that HOTAIR suppresses the osteogenic differentiation of BMSCs.

HOTAIR targets miR-378g

As the effect of HOTAIR on osteogenic differentiation is well known, we expect to elucidate the mechanism of action of HOTAIR. The starBase sharing site revealed the existence of targeting sites for HOTAIR and miR-378g (Figure 4(a)). By using a dual-luciferase assay to verify the results, the luciferase activity was found to decrease after the co-transfection of wild-type HOTAIR and agomiR-378g; however, no significant change was found after the co-transfection

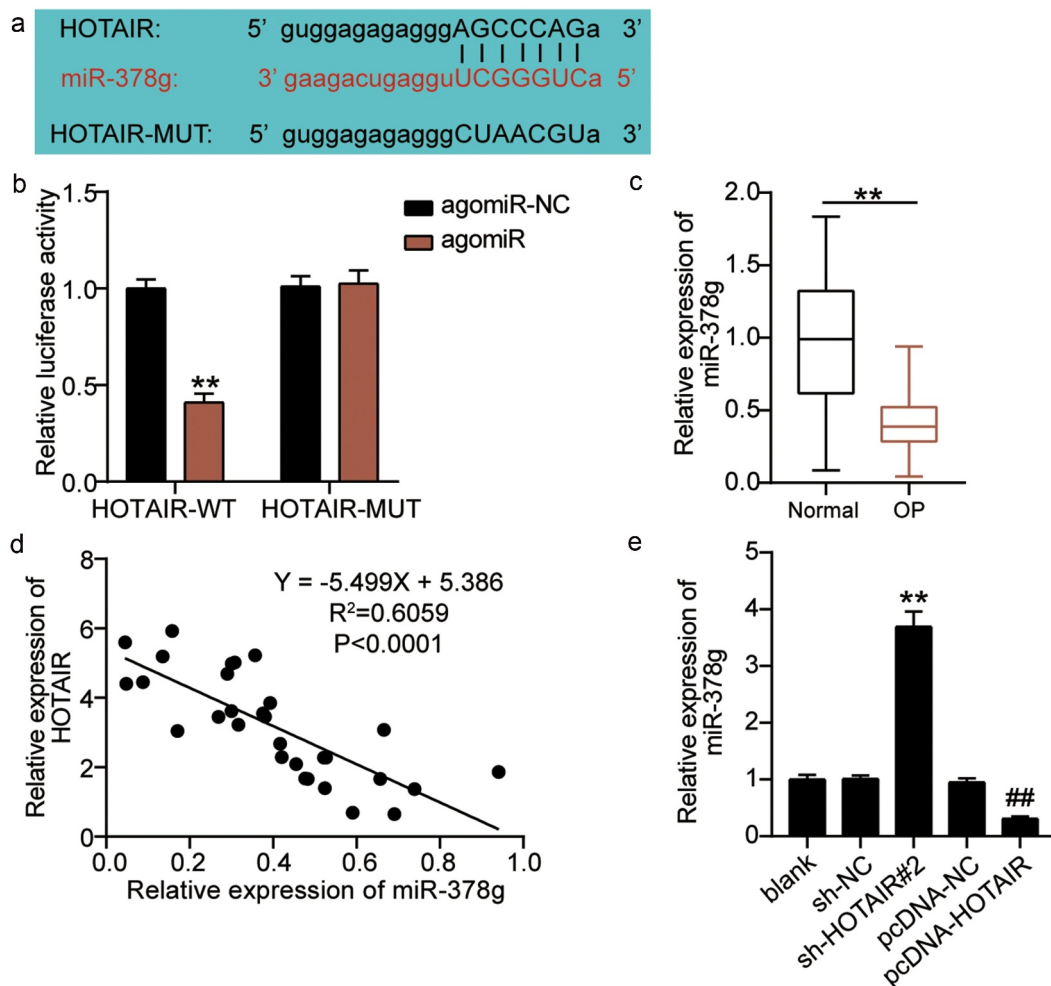


Figure 4. HOTAIR targets miR-378g. (a) Prediction of the binding sites between HOTAIR and miR-378g by starBase. (b) Binding between HOTAIR and miR-378g as assessed by the luciferase activity assay. ** $P < 0.001$ vs. agomiR-NC. (c) miR-378g expression levels in the serum of patients with non-osteoporotic bone fractures (normal) or osteoporosis (OP). ** $P < 0.001$. (d) The correlation between HOTAIR and miR-378g analyzed by Pearson's analysis. (e) The miR-378g expression in BMSCs treated with sh-NC or sh-HOTAIR 2# detected by qRT-PCR. ** $P < 0.001$ vs. sh-NC, ## $P < 0.001$ vs. pcDNA-NC. WT, wild-type; MUT, mutant type; HOTAIR, X-inactive specific transcript; miR-378g, microRNA-378 g; sh-HOTAIR, shRNA of HOTAIR; sh-NC, negative control of shRNA; pcDNA-NC, negative control of HOTAIR overexpression; pcDNA-HOTAIR, HOTAIR overexpression vectors. Data are expressed as mean \pm standard error. In Panels B and E, one-way analysis of variance was used for data analysis, followed by Tukey's post hoc test. In Panel C, unpaired t-test was used for data analysis. The experiment was repeated three times.

of mutant HOTAIR and agomiR-378g (Figure 4(b)). These results proved that HOTAIR targets miR-378g. qRT-PCR was employed to determine serum miR-378g levels. Based on the results, miR-378g levels in osteoporotic patients decreased by nearly 70% compared with those in non-osteoporotic patients (Figure 4(c)). Pearson analysis revealed a negative correlation between HOTAIR and miR-378g expression levels in the serum of OP patients (Figure 4(d)). Additionally, qRT-PCR analysis showed that the expression level of miR-378g increased by approximately 3.7-fold after the downregulation of HOTAIR, and decreased by approximately 70% after the upregulation of HOTAIR (Figure 4(e)), ultimately revealing that HOTAIR targets and negatively regulates miR-378g expression.

HOTAIR restrains osteogenic differentiation by inhibiting miR-378g

We examined the regulatory mechanisms of HOTAIR and miR-378g on osteogenic differentiation. When antago miR-378g was transfected into BMSCs, the HOTAIR level did not change, while the expression level of miR-378g decreased by 70% (Figure 5(a,b)). However, the HOTAIR level was reduced by 75% compared to that of the blank group after the co-downregulation of HOTAIR and miR-378g, while the miR-378g level was similar to that of the blank group (Figure 5(a,b)). Such finding suggests that HOTAIR and miR-378g are co-downregulated. Furthermore, the ALP and RUNX2 levels were found to decrease by approximately 50% and 55%, respectively, after knockdown of miR-378g compared with antagomiR-NC, and the low expression of HOTAIR reduced the inhibitory effect of miR-378g knockdown on ALP and RUNX2 (Figure 5(c,d)). Similarly, Western blotting showed that the levels of ALP and RUNX2 decreased after miR-378g interference, while the co-knockdown of HOTAIR and miR-378g showed no significant changes in the protein levels of ALP and RUNX2 (Figure 5(e)). In addition, ARS staining showed that calcium deposition decreased after transfection with antago miR-378g, and this suppression effect was reversed by knockdown of HOTAIR (figure 5(f)). These

findings indicate that the inhibitory effect of HOTAIR on osteogenic differentiation may be mediated via miR-378g.

miR-378g targets NNMT

miR-378g participates in the regulation of various physiological processes through the negative regulation of its target gene [37]. We proceeded to investigate the downstream target genes of miR-378g. As shown in Figure 6(a), NNMT contains three targets associated with miR-378g. A dual-luciferase assay revealed that compared with agomiR-NC, luciferase activity decreased by 65% after co-transfection of WT and agomiR, and decreased by 55%, 40%, and 30%, respectively, after co-transfection of MUT1, MUT 2, or MUT3, and agomiR. In addition, no significant change in luciferase activity was found after co-transfection with co-MUT and agomiR (Figure 6(b)), revealing miR-378g targeting combined with the NNMT 3'UTR. Moreover, serum monitoring showed that the expression of NNMT in the OP group was significantly upregulated compared to that in the normal group (Figure 6(c)). In addition, Pearson analysis showed that serum NNMT was negatively correlated with the expression of miR-378g in OP patients (Figure 6(d)). Furthermore, the regulatory effects of miR-378g on NNMT were monitored. Western blotting showed that NNMT decreased after miR-378g overexpression, but increased after miR-378g interference (Figure 6(e)). In addition, NNMT mRNA and protein levels decreased in the sh-HOTAIR 2# group compared to those in the sh-NC group or antagomiR + sh-HOTAIR 2# group (Figure 6(f,g)). Such finding indicates that miR-378g negatively regulates NNMT, while HOTAIR reverses this regulatory effect.

miR-378g promotes osteogenic differentiation by inhibiting NNMT

NNMT and miR-378g of BMSCs were downregulated to explore the changes in osteogenic differentiation. NNMT knockdown was transferred to BMSCs with either sh-NNMT #1, sh-NNMT T #2, or sh-NNMT #3, and the level of NNMT was found to decrease by approximately 60%, 50%, and 35%,

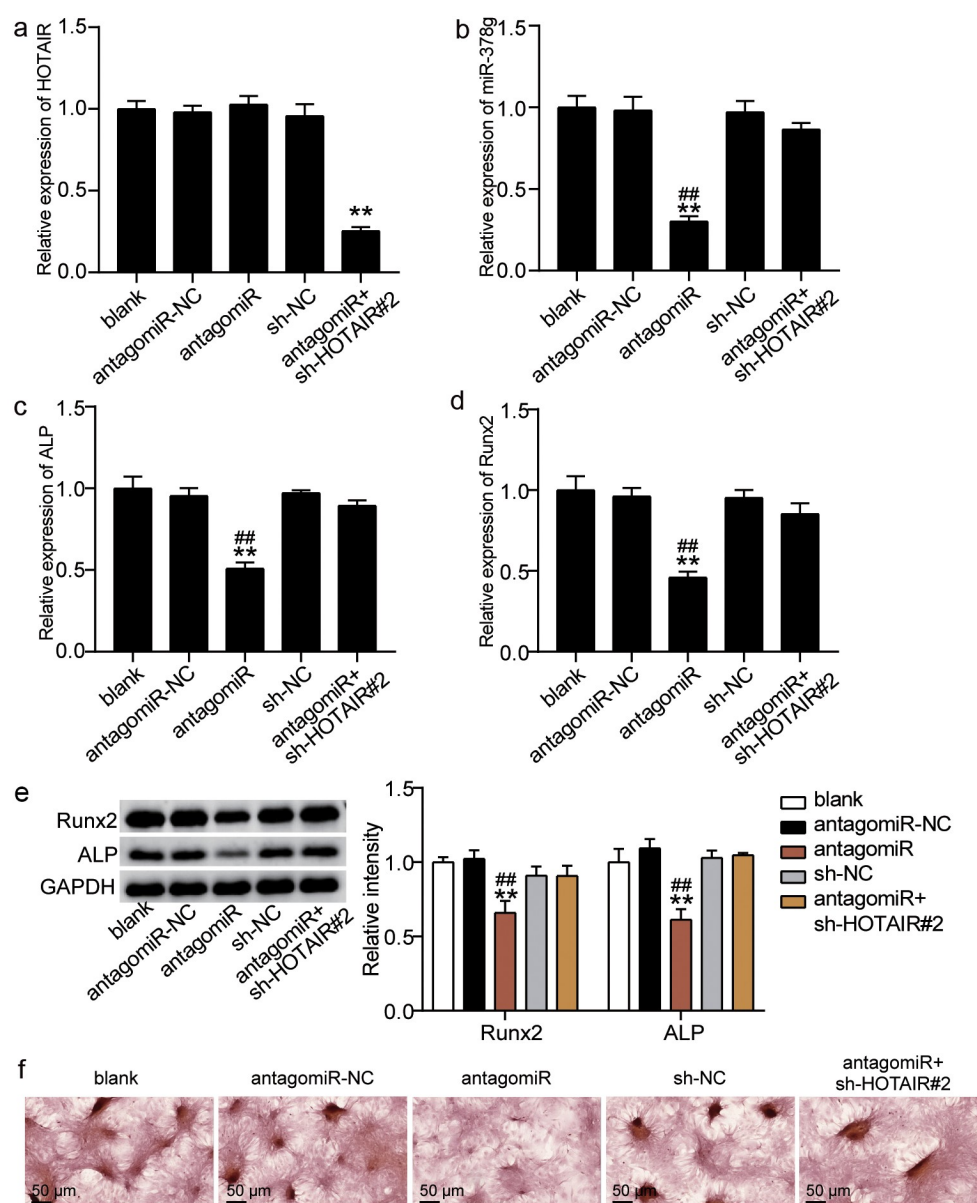


Figure 5. HOTAIR suppresses osteogenesis by inhibiting miR-378g. (a) HOTAIR expression in BMSCs treated with sh-NC, sh-HOTAIR 2#, antagomiR-NC, or antagomiR. (b) miR-378g expression in BMSCs treated with sh-NC, sh-HOTAIR 2#, antagomiR-NC, or antagomiR. (c) ALP expression in BMSCs treated with sh-NC, sh-HOTAIR 2#, antagomiR-NC, or antagomiR. (d) RUNX2 expression in BMSCs treated with sh-NC, sh-HOTAIR 2#, antagomiR-NC, or antagomiR. (e) ALP and RUNX2 protein expression in BMSCs treated with sh-NC, sh-HOTAIR 2#, antagomiR-NC, or antagomiR. (f) The mineralized nodules of BMSCs treated with sh-NC, sh-HOTAIR 2#, antagomiR-NC, or antagomiR measured by Alizarin Red S staining. ** $P < 0.001$ vs. blank. ## $P < 0.001$ vs. sh-HOTAIR#2+ antagomiR. BMSCs, Bone mesenchymal stem cells; HOTAIR, X-inactive specific transcript; ALP, alkaline phosphatase; RUNX2, runt related transcription factor 2. sh-HOTAIR, shRNA of HOTAIR; sh-NC, shRNA of negative control; antagomiR, antago miR-378g; antagomiR-NC antago miR-378g negative control. Data are expressed as mean \pm standard error. One-way analysis of variance was used for data analysis, followed by Tukey's post hoc test. The experiment was repeated three times.

respectively (Figure 7(a)). Sh-NNMT #1 was selected for the follow-up experiments. qRT-PCR showed that miR-378g reversed the effect of NNMT knockdown on NNMT levels (Figure 7(b)). The effect of NNMT on the mRNA expression

levels of ALP and RUNX2 in BMSCs was further studied. ALP and RUNX2 mRNA levels in the sh-NNMT #1 group were 1.8-fold and 2.4-fold higher than levels in the sh-NC group. Further, antago miR-378g partially eliminated the effect of sh-

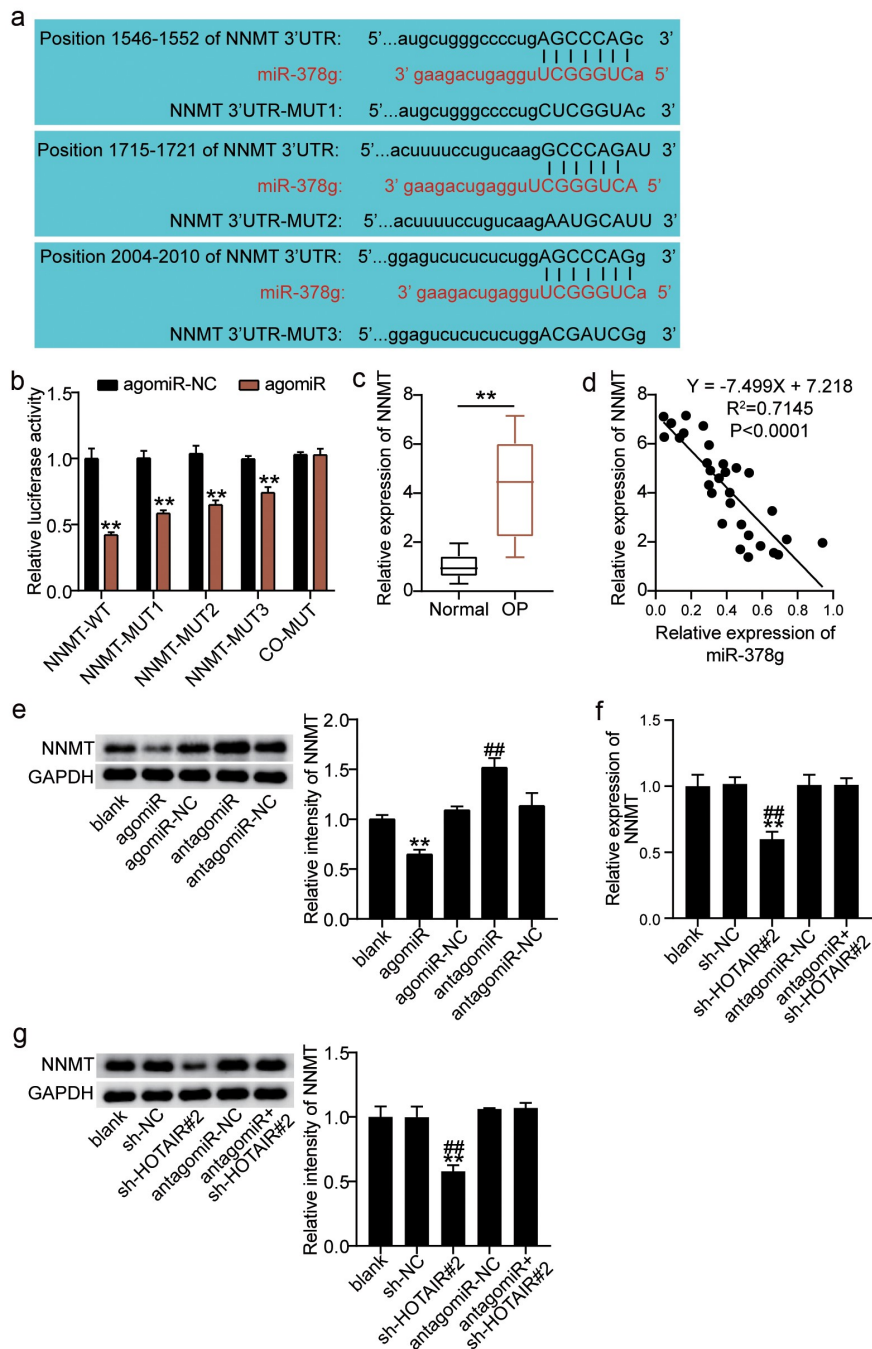


Figure 6. miR-378g targets NNMT mRNA. (a) Prediction of the binding sites between NNMT and miR-378g by TargetScan. (b) The binding between NNMT and miR-378g as assessed by the luciferase activity assay. $^{**}P < 0.001$ vs. agomiR-NC. (c) NNMT mRNA expression levels in the serum of patients with non-osteoporotic bone fractures (normal) or osteoporosis (OP). $^{**}P < 0.001$. (d) The correlation between NNMT and miR-378g assessed using Pearson's analysis. (e) NNMT protein expression in BMSCs treated with agomiR-NC, agomiR, antagomiR-NC, or antagomiR. $^{**}P < 0.001$ vs. agomiR-NC. $^{##}P < 0.001$ vs. antagomiR-NC. (f) NNMT expression in BMSCs treated with sh-NC, sh-HOTAIR 2#, antagomiR-NC, or antagomiR. (g) NNMT protein expression in BMSCs treated with sh-NC, sh-HOTAIR 2#, antagomiR-NC, or antagomiR. (f-g) $^{**}P < 0.001$ vs. sh-NC. $^{##}P < 0.001$ vs. sh-HOTAIR#2+ antagomiR. BMSCs, Bone mesenchymal stem cells; HOTAIR, X-inactive specific transcript; NNMT, Nicotinamide N-methyltransferase. sh-HOTAIR, shRNA of HOTAIR; sh-NC, shRNA of negative control; antagomiR, antago miR-378g; antagomiR-NC antago miR-378g negative control. Data are expressed as mean \pm standard error. One-way analysis of variance was used for data analysis, followed by Tukey's post hoc test. The experiment was repeated three times.

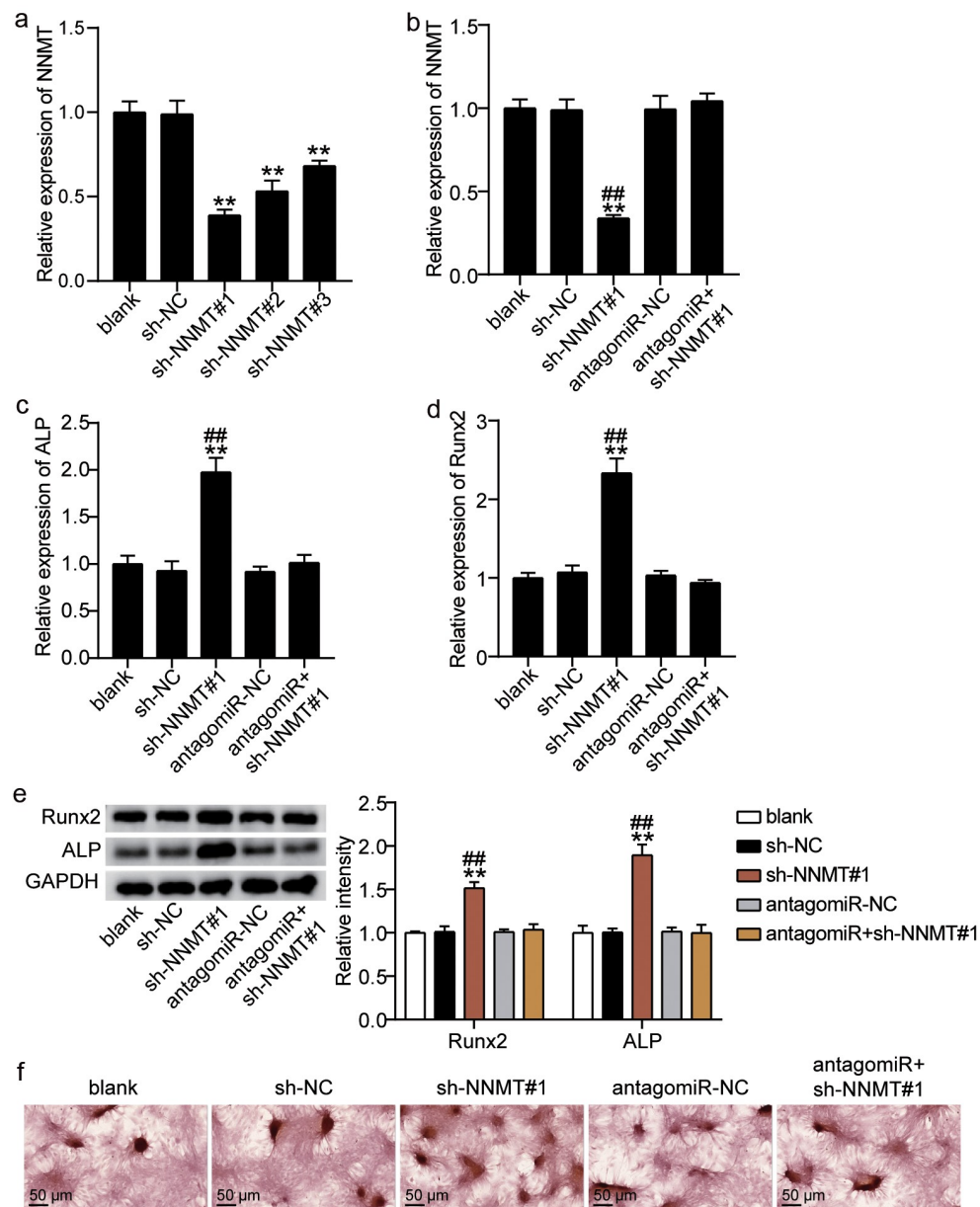


Figure 7. miR-378g enhances osteogenesis by inhibiting NNMT mRNA. (a) NNMT expression in BMSCs treated with sh-NC, sh-NNMT 1#, sh-NNMT 2#, or sh-NNMT 3#. $^{**}P < 0.001$ vs. sh-NC. (b) NNMT expression in BMSCs treated with sh-NC, sh-NNMT 1#, antagomiR-NC, or antagomiR. (c) ALP expression in BMSCs treated with sh-NC, sh-NNMT 1#, antagomiR-NC, or antagomiR. (d) RUNX2 expression in BMSCs treated with sh-NC, sh-NNMT 1#, antagomiR-NC, or antagomiR. (e) ALP and RUNX2 protein expression in BMSCs treated with sh-NC, sh-NNMT 1#, antagomiR-NC, or antagomiR. (b-e) $^{**}P < 0.001$ vs. blank. $^{##}P < 0.001$ vs. sh-NNMT#1+ antagomiR. (f) The mineralized nodules of BMSCs treated with sh-NC, sh-NNMT 1#, antagomiR-NC, or antagomiR measured by Alizarin Red S staining. BMSCs, Bone mesenchymal stem cells; ALP, alkaline phosphatase; RUNX2, runt related transcription factor 2; NNMT, Nicotinamide N-methyltransferase. sh-NNMT, shRNA of NNMT; sh-NC, shRNA of negative control; antagomiR, antago miR-378g; antagomiR-NC antago miR-378g negative control. Data are expressed as mean \pm standard error. One-way analysis of variance was used for data analysis, followed by Tukey's post hoc test. The experiment was repeated three times.

NNMT #1 on ALP and RUNX2 (Figure 7(c,d)). Based on Western blotting, ALP and RUNX2 levels increased by 1.5-fold and 2.0-fold after NNMT knockdown, and were similar to the blank group after knockdown of NNMT and miR-378g (Figure 7

(e)). Additionally, ARS staining showed that the inhibition of NNMT expression increased the degree of calcium nodules, while miR-378g silencing reversed the effect of NNMT knockdown on calcium nodules (figure 7(f)). These results indicate

that miR-378g promotes osteogenic differentiation by targeting NNMT.

Discussion

Dysregulation of osteoblast differentiation is associated with the progression of osteoporosis. Further, ALP, calcium deposition, and RUNX2 levels are often employed to illustrate osteoblast differentiation and its potential for treating OP [38]. In this study, we elucidated the effect of HOTAIR/miR-378g/NNMT on the osteogenic differentiation of BMSCs based on changes in ALP, RUNX2, and calcium deposition levels, thereby providing a potential biomarker for the treatment of OP.

HOTAIR is closely related to bone formation. Zhan et al. [39] found that the overexpression of HOTAIR induced extracellular matrix degradation, apoptosis, and senescence in nucleus pulposus cells. Misawa et al. [40] reported that the downregulation of HOTAIR resulted in the upregulation and increased mineralization of osteosarcoma cells and ALP expression in mineralized medium. In this study, we found that HOTAIR was overexpressed in the serum of OP patients and was underexpressed during the osteogenic differentiation of BMSCs, which align with the findings of Shen et al. [16]. In addition, interference with HOTAIR enhanced the expression of ALP and RUNX2 and promoted calcium deposition in BMSCs. This finding was similar to that observed in osteosarcoma cells by Misawa et al. [40]. Furthermore, this study revealed that HOTAIR upregulation inhibits the osteogenic differentiation of BMSCs, which suggests that HOTAIR may be involved in BMSC-mediated OP.

lncRNAs may act as competing endogenous RNAs (ceRNAs) by competitively binding to miRNAs through their miRNA response elements, thereby regulating the expression levels of miRNAs that target mRNAs [41]. Thus, lncRNAs can act as miRNA sponges, reducing their regulatory effects on mRNAs [42]. Abnormal lncRNA-miRNA-mRNA networks of ceRNAs have been reported to be involved in the development of OP [43]. For example, silencing LNC_000052 inhibited PIK3R1 expression by upregulating miR-96-5p to promote the proliferation,

migration, and osteogenesis of osteoporotic BMSCs and inhibit cell apoptosis [14]. The lncRNA, NEAT1, regulates the expression of OP-related genes (*ALP*, *OCN*, and *OPN*) in BMSCs by regulating the miR-29b-3p-BMP1 axis [44]. miR-378 has been shown to promote BMSC differentiation into osteoclasts in vitro [45]. In addition, another study revealed that miR-378 was underexpressed in high glucose-induced OP mice; however, miR-378 increased ALP activity and promoted RUNX2 expression [46]. This study found that miR-378g expression in the serum of OP patients was downregulated, interference miR-378g inhibited ALP and RUNX2 levels, and reduced calcium deposition, which is similar to the findings of previous studies. The molecular mechanism revealed that miR-378g was negatively regulated by HOTAIR, and interfering with miR-378g eliminated downregulated HOTAIR-induced osteogenesis. HOTAIR exacerbates bone marrow mesenchymal stem cell-mediated osteoporosis through sponging miR-378g.

Accumulating literature suggests that miR-378g can bind to different mRNAs and participate in various physiological processes. For example, Liu et al. [47] reported that miR-378g targeted CHI3L1 to regulate the migration, invasion, and EMT of ovarian cancer cells. Li et al. [48] showed that *HOXC13*, a target gene of miR-378g, accelerates the malignant behavior of oral squamous cell carcinoma cells. Lin et al. [37] revealed that miR-378g partially enhances the radiosensitivity of NPC cells by targeting SHP-1. In this study, miR-378g was found to be a potential miRNA upstream of NNMT by bioinformatics analysis. Moreover, targeting analysis demonstrated that NNMT has a binding site for miR-378g, is a target gene for miR-378g, and is positively regulated by HOTAIR. Interference with NNMT promoted the osteogenic differentiation of BMSCs and reversed the inhibitory effect of miR-378g knockdown on osteogenic differentiation. This finding is consistent with that of Wang et al. [26]. HOTAIR acts as a ceRNA to damage the osteogenic differentiation of BMSCs through the miR-378g/NNMT axis.

This study had some limitations. First, miR-378g/NNMT is not the only regulatory pathway for HOTAIR, and other mechanisms by which

HOTAIR affects OP need to be elucidated. In addition, the effect of HOTAIR on OP needs to be further demonstrated at the animal level.

Conclusion

In summary, HOTAIR was found to be overexpressed in OP. Further downregulation of the ceRNA, NNMT, by miR-378g sponge significantly inhibited the osteogenic differentiation of BMSCs. Therefore, our findings demonstrate that HOTAIR/miR-378g/NNMT is a potential target for the osteogenic differentiation of BMSCs and has a certain value in the diagnosis and treatment of OP.

Highlights

- HOTAIR and NNMT are highly expressed in OP and inhibit BMSC osteogenic differentiation.
- miR-378g alleviates OP by inducing the osteogenic differentiation of BMSCs.
- HOTAIR acts as a ceRNA to damage BMSC osteogenic differentiation via the miR-378g/NNMT axis.

Ethics approval and consent to participate

The present study was approved by the Ethics Committee of Wuhan Hankou Hospital (Wuhan, China). All patients signed written informed consent.

Consent for publication

Consent for publication was obtained from the participants.

Availability of Data and Materials

The datasets used and/or analyzed during the current study are available from the corresponding author on reasonable request.

Disclosure statement

No potential conflict of interest was reported by the authors.

Funding

The authors reported there is no funding associated with the work featured in this article.

Authors' contributions

WW and TL performed the experiments and data analysis. WW and TL conceived and designed the study. TL and SBF made the acquisition of data. SBF did the analysis and interpretation of data. All authors read and approved the manuscript.

References

- [1] Ge DW, Wang WW, Chen HT, et al. Functions of microRNAs in osteoporosis. *Eur Rev Med Pharmacol Sci.* 2017;21(21):4784–4789.
- [2] Lippuner K. [Osteoporosis – a global challenge?]. *Therapeutische Umschau Revue Therapeutique.* 2012;69(3):135–136.
- [3] Miller PD. Management of severe osteoporosis. *Expert Opin Pharmacother.* 2016;17(4):473–488.
- [4] Maluta T, Toso G, Negri S, et al. Correlation between hip osteoarthritis and proximal femoral fracture site: could it be protective for intracapsular neck fractures? A retrospective study on 320 cases. *Osteoporos Int.* 2019;30(8):1591–1596.
- [5] Manolagas SC. From estrogen-centric to aging and oxidative stress: a revised perspective of the pathogenesis of osteoporosis. *Endocr Rev.* 2010;31(3):266–300.
- [6] Yeung DK, Griffith JF, Antonio GE, et al. Osteoporosis is associated with increased marrow fat content and decreased marrow fat unsaturation: a proton MR spectroscopy study. *J Magn Reson Imaging.* 2005;22(2):279–285.
- [7] Jathar S, Kumar V, Srivastava J, et al. Technological developments in lncRNA biology. *Adv Exp Med Biol.* 2017;1008:283–323.
- [8] Kopp F, Mendell JT. Functional classification and experimental dissection of long noncoding RNAs. *Cell.* 2018;172(3):393–407.
- [9] Qian X, Zhao J, Yeung PY, et al. Revealing lncRNA structures and interactions by sequencing-based approaches. *Trends Biochem Sci.* 2019;44(1):33–52.
- [10] Jarroux J, Morillon A, Pinskaya M. History, discovery, and classification of lncRNAs. *Adv Exp Med Biol.* 2017;1008:1–46.
- [11] Schmitz SU, Grote P, Herrmann BG. Mechanisms of long noncoding RNA function in development and disease. *Cell Mol Life Sci.* 2016;73(13):2491–2509.
- [12] Li D, Yang C, Yin C, et al. LncRNA, important player in bone development and disease. *Endocr Metab Immune Disord Drug Targets.* 2020;20(1):50–66.
- [13] Tang S, Xie Z, Wang P, et al. LncRNA-OG promotes the osteogenic differentiation of bone marrow-derived mesenchymal stem cells under the regulation of hnRNPK. *Stem Cells.* 2019;37(2):270–283.
- [14] Sun X, Shen H, Liu S, et al. Long noncoding RNA SNHG14 promotes the aggressiveness of retinoblastoma by sponging microRNA-124 and thereby upregulating STAT3. *Int J Mol Med.* 2020;45(6):1685–1696.

- [15] Rajagopal T, Talluri S, Akshaya RL, et al. HOTAIR lncRNA: a novel oncogenic propellant in human cancer. *Clin Chim Acta*. 2020;503:1–18.
- [16] Shen JJ, Zhang CH, Chen ZW, et al. LncRNA HOTAIR inhibited osteogenic differentiation of BMSCs by regulating Wnt/ β -catenin pathway. *Eur Rev Med Pharmacol Sci*. 2019;23(17):7232–7246.
- [17] Bryden WL. Circulating levels of biotin in the fowl (*Gallus domesticus*): modulation by oestrogen. *Comp Biochem Physiol Comp Physiol*. 1988;91(4):773–777.
- [18] Thomson DW, Dinger ME. Endogenous microRNA sponges: evidence and controversy. *Nat Rev Genet*. 2016;17(5):272–283.
- [19] Yang Y, Yujiao W, Fang W, et al. The roles of miRNA, lncRNA and circRNA in the development of osteoporosis. *Biol Res*. 2020;53(1):40.
- [20] Zhang L, Tang Y, Zhu X, et al. Overexpression of MiR-335-5p promotes bone formation and regeneration in mice. *J Bone Miner Res*. 2017;32(12):2466–2475.
- [21] Liu H, Dong Y, Feng X, et al. miR-34a promotes bone regeneration in irradiated bone defects by enhancing osteoblastic differentiation of mesenchymal stromal cells in rats. *Stem Cell Res Ther*. 2019;10(1):180.
- [22] Kahai S, Lee SC, Lee DY, et al. MicroRNA miR-378 regulates nephronectin expression modulating osteoblast differentiation by targeting GalNT-7. *PloS One*. 2009;4(10):e7535.
- [23] Bian Y, Qian W, Li H, et al. Pathogenesis of glucocorticoid-induced avascular necrosis: a microarray analysis of gene expression in vitro. *Int J Mol Med*. 2015;36(3):678–684.
- [24] Gao Y, van Haren MJ, Moret EE, et al. Bisubstrate inhibitors of nicotinamide N-methyltransferase (NNMT) with enhanced activity. *J Med Chem*. 2019;62(14):6597–6614.
- [25] Agrawal Singh S, Lerdrup M, Gomes AR, et al. PLZF targets developmental enhancers for activation during osteogenic differentiation of human mesenchymal stem cells. *eLife*. 2019;8.
- [26] Wang H, Zhou K, Xiao F, et al. Identification of circRNA-associated ceRNA network in BMSCs of OVX models for postmenopausal osteoporosis. *Sci Rep*. 2020;10(1):10896.
- [27] Zhou R, Miao S, Xu J, et al. Circular RNA circ_0000020 promotes osteogenic differentiation to reduce osteoporosis via sponging microRNA miR-142-5p to up-regulate bone morphogenetic protein BMP2. *Bioengineered*. 2021;12(1):3824–3836.
- [28] Hu H, Zhao C, Zhang P, et al. miR-26b modulates OA induced BMSC osteogenesis through regulating GSK3 β / β -catenin pathway. *Exp Mol Pathol*. 2019;107:158–164.
- [29] Hu N, Feng C, Jiang Y, et al. Regulatory effect of Mir-205 on osteogenic differentiation of bone mesenchymal stem cells (BMSCs): possible role of SATB2/Runx2 and ERK/MAPK pathway. *Int J Mol Sci*. 2015;16(5):10491–10506.
- [30] Yang X, Yang J, Lei P, et al. LncRNA MALAT1 shuttled by bone marrow-derived mesenchymal stem cells-secreted exosomes alleviates osteoporosis through mediating microRNA-34c/SATB2 axis. *Aging (Albany NY)*. 2019;11(20):8777–8791.
- [31] Zhao W, Geng D, Li S, et al. HOTAIR influences cell growth, migration, invasion, and apoptosis via the miR-20a-5p/HMGA2 axis in breast cancer. *Cancer Med*. 2018;7(3):842–855.
- [32] Xiang Y, Zhang Y, Xia Y, et al. LncRNA MEG3 targeting miR-424-5p via MAPK signaling pathway mediates neuronal apoptosis in ischemic stroke. *Aging (Albany NY)*. 2020;12(4):3156–3174.
- [33] Li F, Wu H, Zou G, et al. Circular RNA_0062582 promotes osteogenic differentiation of human bone marrow mesenchymal stem cells via regulation of microRNA-145/CBFB axis. *Bioengineered*. 2021;12(1):1952–1963.
- [34] Chen E, Liu G, Zhou X, et al. Concentration-dependent, dual roles of IL-10 in the osteogenesis of human BMSCs via P38/MAPK and NF- κ B signaling pathways. *FASEB J*. 2018;32(9):4917–4929.
- [35] Zhang P, Wu Y, Jiang Z, et al. Osteogenic response of mesenchymal stem cells to continuous mechanical strain is dependent on ERK1/2-Runx2 signaling. *Int J Mol Med*. 2012;29(6):1083–1089.
- [36] Li C, Wei G, Gu Q, et al. Donor age and cell passage affect osteogenic ability of rat bone marrow mesenchymal stem cells. *Cell Biochem Biophys*. 2015;72(2):543–549.
- [37] Lin T, Zhou F, Zhou H, et al. MicroRNA-378g enhanced radiosensitivity of NPC cells partially by targeting protein tyrosine phosphatase SHP-1. *Int J Radiat Biol*. 2015;91(11):859–866.
- [38] Zhu H, Chen H, Ding D, et al. The interaction of miR-181a-5p and sirtuin 1 regulated human bone marrow mesenchymal stem cells differentiation and apoptosis. *Bioengineered*. 2021;12(1):1426–1435.
- [39] Zhan S, Wang K, Song Y, et al. Long non-coding RNA HOTAIR modulates intervertebral disc degenerative changes via Wnt/ β -catenin pathway. *Arthritis Res Ther*. 2019;21(1):201.
- [40] Misawa A, Orimo H. LncRNA HOTAIR inhibits mineralization in osteoblastic osteosarcoma cells by epigenetically repressing ALPL. *Calcif Tissue Int*. 2018;103(4):422–430.
- [41] Salmena L, Poliseno L, Tay Y, et al. A ceRNA hypothesis: the rosetta stone of a hidden RNA language? *Cell*. 2011;146(3):353–358.
- [42] Paraskevopoulou MD, Hatzigeorgiou AG. Analyzing MiRNA-LncRNA Interactions. *Methods Mol Biol*. 2016;1402:271–286.
- [43] Zhang X, Liang H, Kourkoumelis N, et al. Comprehensive analysis of lncRNA and miRNA expression profiles and ceRNA network construction in osteoporosis. *Calcif Tissue Int*. 2020;106(4):343–354.

- [44] Zhang Y, Chen B, Li D, et al. LncRNA NEAT1/miR-29b-3p/BMP1 axis promotes osteogenic differentiation in human bone marrow-derived mesenchymal stem cells. *Pathol Res Pract.* 2019;215(3):525–531.
- [45] Liu S, Wang C, Bai J, et al. Involvement of circRNA_0007059 in the regulation of postmenopausal osteoporosis by promoting the microRNA-378/BMP-2 axis. *Cell Biol Int.* 2021;45(2):447–455.
- [46] You L, Gu W, Chen L, et al. MiR-378 overexpression attenuates high glucose-suppressed osteogenic differentiation through targeting CASP3 and activating PI3K/Akt signaling pathway. *Int J Clin Exp Pathol.* 2014;7(10):7249–7261.
- [47] Liu W, Yang YJ, An Q. LINC00963 promotes ovarian cancer proliferation, migration and EMT via the miR-378g /CHI3L1 axis. *Cancer Manag Res.* 2020;12:463–473.
- [48] Li W, Zhu Q, Zhang S, et al. HOXC13-AS accelerates cell proliferation and migration in oral squamous cell carcinoma via miR-378g/HOXC13 axis. *Oral Oncol.* 2020;111:104946.